ORIGINAL ARTICLE

Synthesis and characterization of flower-like ZnSe nanostructured thin films by chemical bath deposition (CBD) method

G. Bakiyaraj · R. Dhanasekaran

Abstract Flower-like zinc selenide nanostructured thin films were successfully prepared by a chemical bath deposition method on non-conducting glass substrate in an aqueous alkaline medium using sodium selenosulphate as Se^{2-} ion source. The as-deposited films have been characterized by X-ray diffraction (XRD), high resolution scanning electron microscopy (HRSEM), energy-dispersive X-ray analysis (EDX), optical absorption, and photoluminescence spectroscopy (PL). The XRD studies reveal that the as-deposited ZnSe thin film is nanocrystalline with a face-centered cubic phase. SEM image shows the tens to hundreds of petals are self-assembled within a single nanoflower. The direct optical band gap 'E_g' for as-deposited flower-like ZnSe thin films is found to be 2.80 eV. Room temperature PL measurement indicates that the as-deposited cubic ZnSe thin films have a near band edge (NBE) emission peaked at around 440 nm (2.81 eV) and broad weak band emission peak from 552 nm (2.24 eV) to 658 nm (1.88 eV). The strong NBE emission from the flower-like ZnSe nanostructured thin films reveals their potential as building for optoelectronic devices.

Keywords Semiconductor thin films ·
Nanostructured materials · Chemical bath deposition ·
Structural properties · Optical properties

Introduction

In recent years, there has been considerable interest in the growth and characterization of nanostructured materials due to their significant potential application and novel properties. Various nanostructures of different materials such as nanoparticles, nanorods, and nanowires have already been investigated for solar cells (Goodey et al. 2007; Hsu et al. 2008; Tian et al. 2007). Some nanostructures have insufficient internal surface area, while others are not favorable for light harvesting. Nanoflower morphology with random branches helps overcome these problems partially, while offering good electron transportation (Dhas et al. 2008; Pan et al. 2001). CdS, one of the very important II–VI group semiconductors, plays an important role in the buffer layer in $Cu(In,Ga)(S,Se)_2$ based solar cells. However, Cd is toxic, for industrial production and for environmental protection, it is necessary to replace CdS by an alternative non-toxic buffer layer, which in addition is more transparent in the blue spectral range. Zinc selenide (ZnSe) is an n-type semiconducting material with wide band gap (2.7 eV) and large exciton binding energy of 21 meV, which is a promising candidate for the replacement of the toxic CdS in the buffer layer and good lattice match with $Cu(In,Ga)(S,Se)_2$ (Ahn et al. 2008; Hariskos et al. 2005). Inspired by this, several groups have prepared a series of ZnSe nanostructures with various methods, such as solvothermal method (Yang et al. 2009), chemical vapour deposition (CVD) (Philipose et al. 2007a), metal–organic chemical vapour deposition (MOCVD) (Zhang et al. 2005), molecular beam epitaxy (MBE) (Aichele et al. 2008), pulsed laser deposition (PLD) (Zhang et al. 2007b), laser ablation deposition (ALD) (Solanki et al. 2002), sputtering (Morales et al. 2007), template method (Karanikolos et al. 2005), thermal evaporation (Ashraf et al. 2011), chemical bath deposition (CBD) (Lokhande et al. 1998), and so on. Among them, CBD provides a more promising option due to its simpleness, practicality, large-scale controllability, and low cost. From the literature

G. Bakiyaraj · R. Dhanasekaran (✉)
Crystal Growth Centre, Anna University, Chennai 600025, India
e-mail: rdhanasekaran@annauniv.edu; rdcgc@yahoo.com

survey, there are no reports available on the preparation of ZnSe flower-like nanostructure via CBD. In the present communication, we report the synthesis of a novel shape of ZnSe flower-like nanostructure thin films through a simple CBD method. These nanoflowers are composed of petals layer by layer, which form flower-like shapes. X-ray diffraction, high resolution scanning electron microscopy, energy-dispersive X-ray analysis, optical absorption, and photoluminescence spectrum studies were carried out to investigate the structure, surface, composition, and optical properties of the obtained samples.

Experimental procedure

Substrate cleaning and reagents

The substrate cleaning is very important in the deposition of thin films. Commercially available glass slides with a size of 75 mm × 25 mm × 1.35 mm were used. Before deposition, the glass substrates were cleaned first by a mild soap solution, then degreased with acetone, etched with 5% of HCl for 30 min, and ultrasonically cleaned by de-ionized water and finally dried in air.

Chemicals used for the deposition of ZnSe thin films were analytical grade zinc acetate ($Zn(CH_3CO_2)_2$), hydrazine hydrate (H_6N_2O), 25% liquor ammonia (NH_4OH), sodium hydroxide (NaOH), selenium metal powder, and sodium sulphite (Na_2SO_3) obtained from Merck and directly employed without further purification.

Preparation of Na_2SeSO_3 solution

All solutions were prepared using double-distilled water. The sodium selenosulfate (Na_2SeSO_3) solution was prepared by refluxing 5 g of Se metal powder and 15 g of Na_2SO_3 in 200 ml distilled water for 9 h at 90 °C. It was sealed and kept overnight, since on cooling, a little selenium separated from the solution, which was then filtered to obtain a clear solution of Na_2SeSO_3.

Deposition of ZnSe thin films

For the deposition of ZnSe thin films, 45 ml of 0.5 M aqueous solution of ($Zn(CH_3CO_2)_2$) was taken in a 250 ml capacity glass beaker, and 2 ml of hydrazine hydrate was added with constant stirring. To this, the liquor ammonia was added drop-by-drop with constant stirring. At the beginning, the solution appears to be cloudy due to the formation of $Zn(OH)_2$. In addition to excess ammonia, the white precipitate of zinc hydroxide is dissolved and made the solution clear and transparent. The pH of the solution was adjusted to 11 by adding NaOH (1 M) solution. The

temperature of the solution was then allowed to rise slowly with constant stirring. After reaching the required temperature of 75 °C, 45 ml of freshly prepared Na_2SeSO_3 was added with constant stirring. A cleaned glass substrate was positioned vertically on a specially designed substrate holder and rotated in the reactive solution at a speed of 100 ± 5 rpm. The deposition of ZnSe on the substrate takes place and the period of deposition is 2½ h. The substrate was subsequently removed from the beaker. The films obtained were washed with distilled water, dried in air, preserved in an airtight plastic container, and kept in a desiccator.

Characterization

Film thickness (175 nm) was measured using Filmetrics measurement system. The crystalline structure of the films was studied by X-ray diffraction measurements obtained with a Rigaku X-Ray Diffractometer in the 2θ range of 10°–80° using CuK_α radiation of wavelength $\lambda = 1.5406$ Å. The X-ray tube was operated at 40 kV (voltage) and 30 mA (current) with scanning speed of 0.5°/min. The chemical compositions, as well as the morphology of the ZnSe thin films were observed with HRSEM (model FEI QUANTA 200F) equipped with EDX facility. Absorption spectra were recorded with a Shimadzu UV-1601PC spectrophotometer at normal incidence. All the measurements were made at room temperature with a blank glass substrate in the reference beam path. Photoluminescence measurement was performed at room temperature using a Perkin-Elmer LS-55 luminescence spectrometer with excitation wavelength of 380 nm.

Results and discussion

Structural analysis

Figure 1 shows the X-ray diffraction pattern of chemically deposited flower-like ZnSe nanostructured thin films on glass substrate. The diffraction peaks are indexed to the face-centered cubic phase of ZnSe with lattice constants of $a = 5.618$ Å [Joint Committee on Powder Diffraction Standards (JCPDS) card number 80-0021]. It is seen from the spectrum that the flower-like ZnSe thin films exhibited the orientations along (111), (220), and (311) planes corresponding to the 2θ values of angles 27.34°, 45.70°, and 53.82°, respectively. The XRD peak intensity of the (111) plane was relatively higher than those of other reflections. No peaks related to Zn, ZnO, and other zinc compounds are observed. The absence of impurity peaks suggests the high purity of the ZnSe product. Compared with those of the bulk counterpart, the
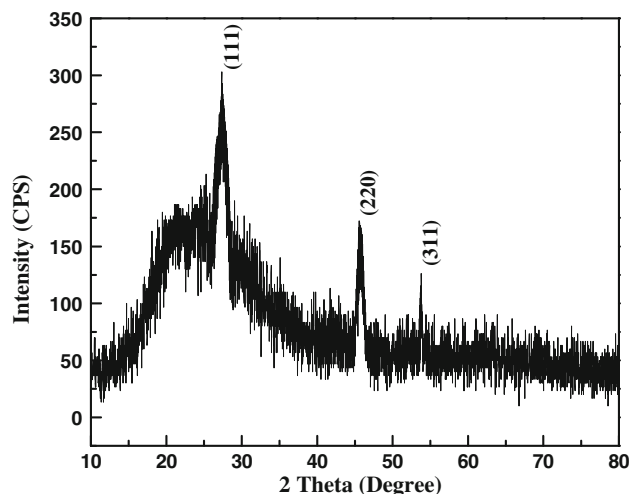
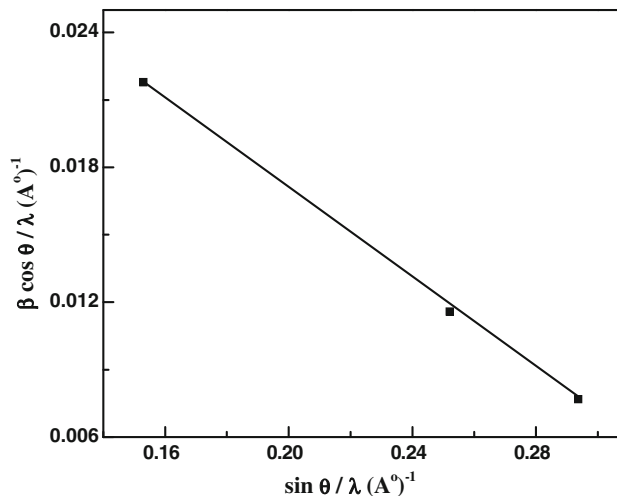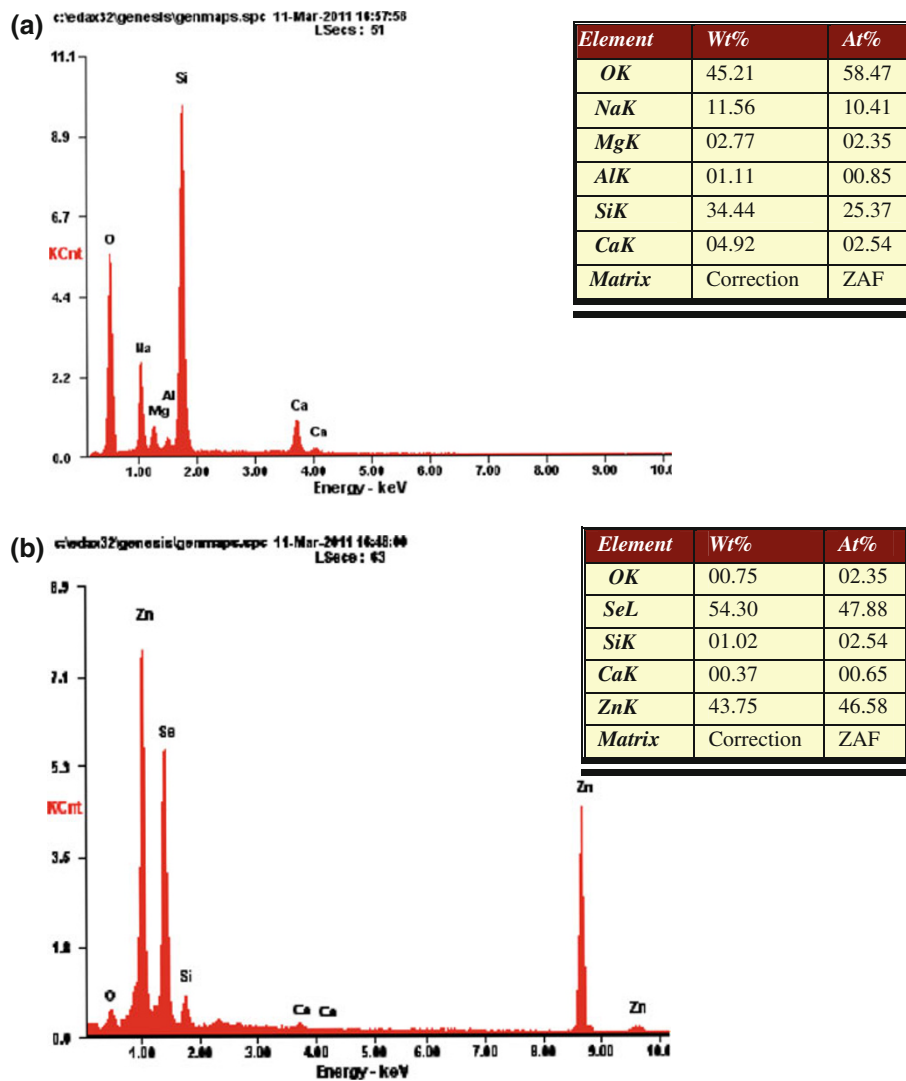**Fig. 1** The X-ray diffraction pattern of flower-like ZnSe nanostructured thin films

Fig. 2 Williamson–Hall plot to determine the particle size and strain of flower-like ZnSe nanostructured thin films

peaks are relatively broadened, which further indicates that the nanoflowers have very small crystallite size. The obtained d values were compared with the powder diffraction data file. Table 1 shows the comparison of the d values obtained from XRD with JCPDS data. Peak broadening may also be caused by other reasons, such as inhomogeneous strains, twinned structure, lattice bending, or other point defects that may be present in the flower; hence Scherrer's equation may produce results that are different from the actual size (Cullity 1978). In order to calculate the strain (ε) and the particle size (L) of the deposited films, the following relation has been used (Williamson and Hall 1953):

$$\beta \cos \theta/\lambda = 1/L + \varepsilon \sin \theta/\lambda \qquad (1)$$

where β is the full width at half maximum (FWHM) of the diffraction peaks, λ is the wavelength of the X-ray source, and θ is the Bragg's angle. Figure 2 represents the plot of $\beta \cos \theta/\lambda$ versus $\sin \theta/\lambda$ for as-deposited ZnSe thin films samples. The reciprocal of intercept on the y axis gives the average particle size, and the slope of the plot gives the amount of residual strain. Values of 2.702 nm and 10.3444×10^{-2} are obtained for the average grain size and strain, respectively.

Table 1 The comparison of d values, which obtained from XRD and JCPDS data file (80-0021)

d_{XRD} (Å)	d_{JCPDS} (Å)	hkl
3.2580	3.2435	111
1.9830	1.9862	220
1.7020	1.6938	311

Composition and surface morphology analysis

Figure 3a shows the EDX spectrum for blank soda-lime glass substrate. It shows that the glass substrate contains O, Na, Mg, Al, Si, and Ca elements. Figure 3b shows the EDX spectrum of flower-like ZnSe nanostructured thin films, which displays selenium $L_{\alpha 1}$ and $L_{\beta 1}$ (1.64 keV) peaks and zinc $K_{\alpha 1}$ (8.66 keV), and $K_{\beta 1}$ (9.60 keV) peaks. The quantification calculation shows that the atomic ratio of Se:Zn is about 47.88:46.58. The other elements such as O, Si, and Ca are from the glass substrates.

HRSEM observation revealed that numerous well-distributed flower-like nanostructures formed on the film surface. The typical HRSEM images are depicted in Fig. 4a–c. The film is essentially an array of particles that are like flowers. Each particle is a well-formed flower and covered on glass substrate without pinhole and creak. The size of each nanoflower is approximately in the range 100–200 nm and is shown in Fig. 4b. Figure 4c shows a closer view of few such flowers. Each flower is composed of tens to hundreds of petals as shown in Fig. 4b, c. The "petals" of the flowers are much thinner, with a thickness of about 5–10 nm. Meanwhile, due to their thinner petals, leading to much more surface areas, the particles are conjugated to each other. For flower-like ZnSe thin films, the crystallites are self-organized into spherical assembles with protruding petals with puffy flower-like structure. The nanoflowers reported here obviously differ from the flower-like CdS nanostructures, formed via connection of sword-like nanorods (Zhang et al. 2007a). To the best of our knowledge, this is the first time that such fascinating nanostructures of ZnSe have been reported hitherto. From the X-ray diffraction pattern, it is possible to conclude that

Fig. 3 The EDX spectrum of **a** blank soda-lime glass and **b** flower-like ZnSe nanostructured thin films

(a) c:\edax32\genesis\genmaps.spc 11-Mar-2011 16:57:58
LSecs: 51

Element	Wt%	At%
OK	45.21	58.47
NaK	11.56	10.41
MgK	02.77	02.35
AlK	01.11	00.85
SiK	34.44	25.37
CaK	04.92	02.54
Matrix	Correction	ZAF

(b) c:\edax32\genesis\genmaps.spc 11-Mar-2011 16:48:40
LSecs: 63

Element	Wt%	At%
OK	00.75	02.35
SeL	54.30	47.88
SiK	01.02	02.54
CaK	00.37	00.65
ZnK	43.75	46.58
Matrix	Correction	ZAF

these ZnSe nanoflower structures grow preferentially along the (111) planes and provide reactive edge sites to the flower-like arrays.

Optical studies

Optical studies were performed by measuring the absorption of the films deposited on glass substrates in the wavelength range 400–800 nm by subtracting the absorption of the glass substrate, which was taken as a reference. Figure 5 shows the absorption spectrum for flower-like ZnSe nanostructured thin films. It is observed that the absorption edge of the as-deposited ZnSe thin films are red shifted from the absorption edge of the bulk ZnSe. It is indicating the formation of nanostructured flower-like ZnSe thin films. From the absorption data, nearly at the fundamental absorption edge, the values of absorption

coefficient (α) are calculated in the region of strong absorption using the relation (Tarey and Raju 1985):
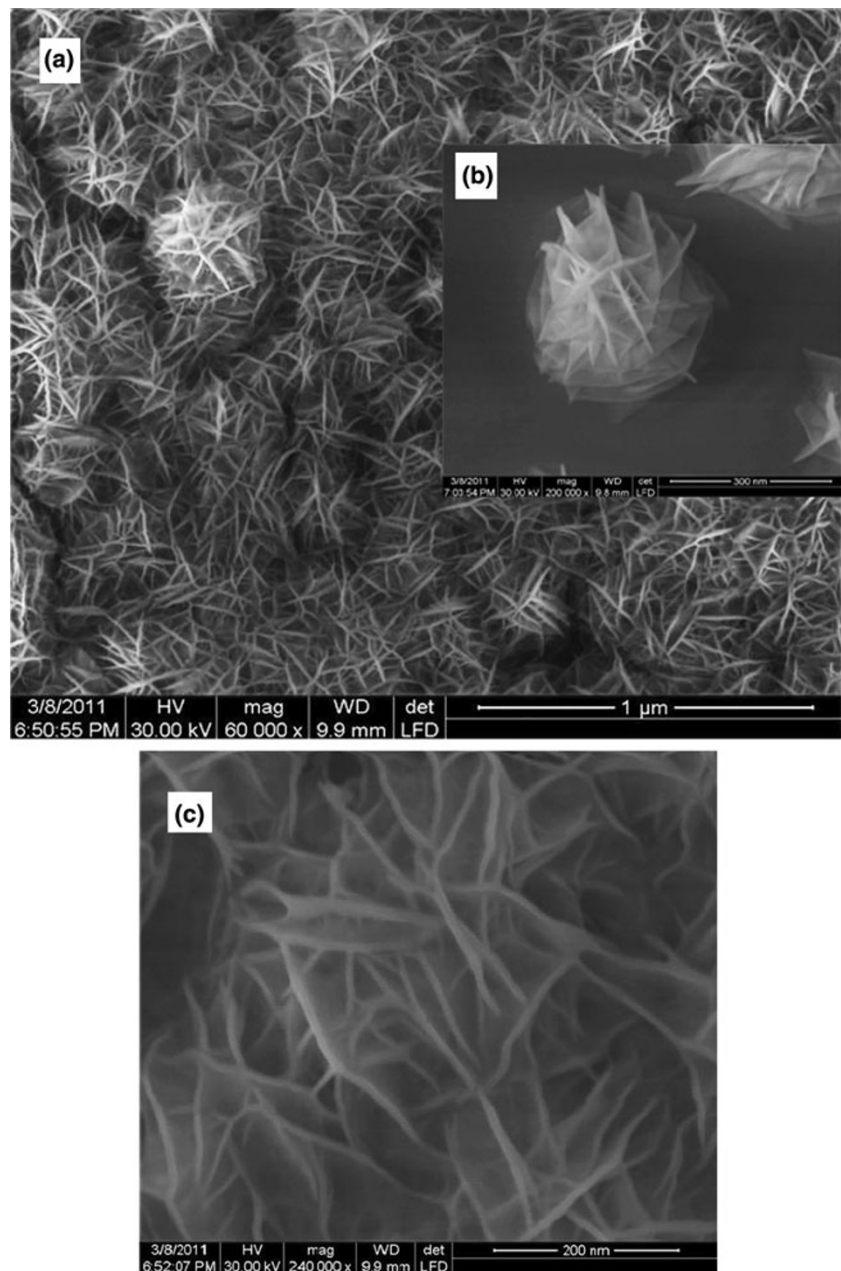
$$\alpha = -(1/t)\ln(T) \qquad (2)$$

where T is the transmission in % and t is the film thickness. The optical band gap E_g has been calculated using Tauc's (Tauc et al. 1966) formula

$$(\alpha h\upsilon)^{1/n} = A(h\upsilon - E_g) \qquad (3)$$

where α is absorption coefficient, $h\upsilon$ is incident photon energy, A is a constant, and the exponent n depends on the type of transition. n may have values ½, 2, 3/2, and 3 corresponding to the allowed direct, allowed indirect, forbidden direct, and forbidden indirect transitions, respectively. Since ZnSe is a direct band-gap material, the corresponding E_g is obtained with $n = 1/2$. The band gap is calculated by extrapolating the linear region of the plot of

Fig. 4 SEM image of flower-like ZnSe nanostructure **a** low magnification view, **b**, **c** high magnification view

$(\alpha h\upsilon)^2$ versus $h\upsilon$ on the energy axis, as shown in inset of Fig. 5. The band-gap values are estimated to be 2.80 eV for ZnSe thin films. These band-gap values are higher than that of bulk values of ZnSe (2.7 eV at 300 K). The enhancement of band gap is attributed to the quantum size effect.

Photoluminescence measurement

A typical room temperature PL spectrum of flower-like ZnSe nanostructured thin films is shown in Fig. 6. In ZnSe, Zn vacancies and Se interstitials introduce energy levels closer to the edge of the valence band edge and hence act as acceptor states, while Se vacancies and Zn interstitials introduce levels closer to the conduction band edge and as donor states (Philipose et al. 2007b; Singh and Chauhan 2009). Absorption of photons can generate electrons and holes. These electrons were trapped in different interstitial sites and vacancies. The as-deposited ZnSe nanoflower has three emission peaks: a strong green emission peak centered at 440 nm (2.81 eV) and one broad weak emission peak in green–red emission region are also observed from 552 nm (2.24 eV) to 658 nm (1.88 eV). The strong green emission is the characteristic of NBE emission of ZnSe. The broad green–red emission band extending from around 552 nm (2.24 eV) to 658 nm (1.88 eV) is a typical deep defect (DD) related emission. This is usually associated
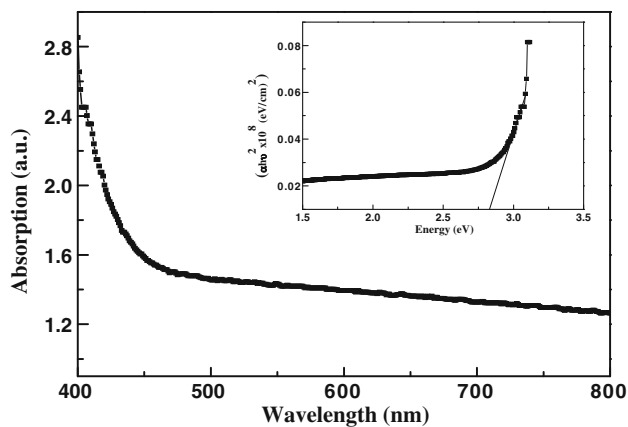
Fig. 5 The variation of optical absorbance versus wavelength of ZnSe thin film [*inset* shows the variation of $(\alpha h\upsilon)^2$ versus $h\upsilon$ to determine the band gap of ZnSe thin films]
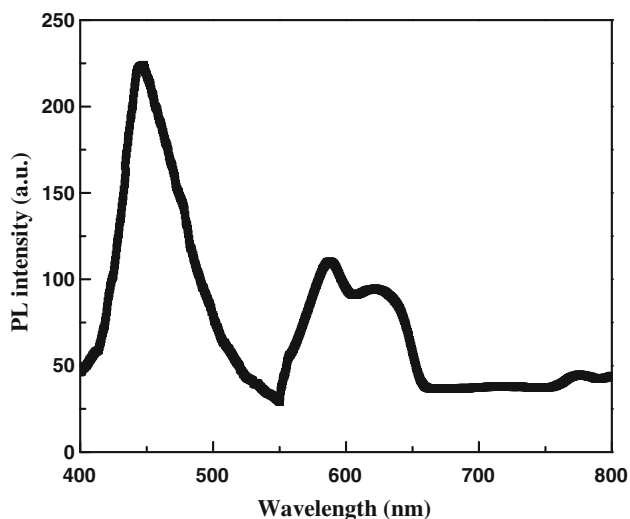

Fig. 6 PL spectra of flower-like ZnSe nanostructured thin films

with dislocation, stacking faults, and non-stoichiometric defects (Zhang et al. 2001). As confirmed by EDX analysis (Fig. 3b), Se atoms are a trace of excess in the ZnSe nanoflowers. Therefore, we deduce that the origin of the green–red emission may be attributed to intrinsic point defect. The intrinsic point defect including the vacancies and interstitials having different charged states introduce different localized energy levels within the band gap and also combine into donor–acceptor pairs (DAPs). The green–red emission peaks extended from 552 nm (2.24 eV) to 658 nm (1.88 eV) by the PL lines attributed to I_{se} or/and V_{zn}. The strong NBE emission and relatively weak deep level emission indicate the ZnSe nanoflower with few defects.

Conclusion

In conclusion, the flower-like ZnSe nanostructures have been prepared by CBD method. Considering the convenience and simplicity of the process and apparatus used, the low-temperature CBD method will present a wide range of possibilities for further development of large-scale production of ZnSe nanomaterials. It was confirmed from X-ray diffraction analysis that the as-deposited films exhibited a nanocrystalline nature and face-centered cubic structure. Surface morphology showed flower-like ZnSe consisting tens to hundreds of self-assembled petals. The number of petal layers gradually decreased towards the edges, resulting in uniquely thin edges, typically <10 nm. Optical band-gap studies indicated that the band gap of as-deposited sample has blue-shift with respect to the corresponding value for the bulk ZnSe material. PL measurements show a strong near band edge emission and relatively weak deep level emissions indicate the flower-like ZnSe nanostructures with few defects.

References

Ahn BT, Larina L, Kim KH, Ahn SJ (2008) Development of new buffer layers for Cu(In, Ga)Se2 solar cells. Pure Appl Chem 80:2091–2102

Aichele T, Tribu A, Bougerol C, Kheng K, André R, Tatarenko S (2008) Defect-free ZnSe nanowire and nanoneedle nanostructure Appl Phys Lett 93:143106(1)–143106(3)

Ashraf M, Akhtar SMJ, Khan AF, Ali Z, Qayyum A (2011) Effect of annealing on structural and optoelectronic properties of nano-structured ZnSe thin films. J Alloys Compd 509:2414–2419

Cullity BD (1978) Elements of X-rays diffraction. Addison–Wesley, London

Dhas V, Muduli S, Lee W, Han S, Ogale S (2008) Enhanced conversion efficiency in dye-sensitized solar cells based on ZnO bifunctional nanoflowers loaded with gold nanoparticles. Appl Phys Lett 93:243108

Goodey AP, Eichfeld SM, Lew K, Redwing JM, Mallouk TE (2007) Silicon nanowire array photoelectrochemical cells. J Am Chem Soc 129:12344–12345

Hariskos D, Spiering S, Powalla M (2005) Buffer layers in Cu(In, Ga)Se2 solar cells and modules. Thin Solid Films 480–481: 99–109

Hsu YF, Xi YY, Djurišić AB, Chan WK (2008) ZnO nanorods for solar cells: hydrothermal growth versus vapor deposition. Appl Phys Lett 92:133507

Karanikolos GN, Alexandridis P, Mallory R, Petrou A, Mountziaris TJ (2005) Templated synthesis of ZnSe nanostructures using lyotropic liquid crystals. Nanotechnology 16:2372–2380

Lokhande CD, Patil PS, Ennaoui A, Tributsch H (1998) Chemical bath ZnSe thin films: deposition and characterization. Appl Surf Sci 123:294–297

Morales M, Vivet N, Levalois M, Bardeau JF (2007) Optimization of ZnSe–SiO$_2$ nanostructures deposited by radio-frequency magnetron sputtering: correlations between plasma species and thin film composition, structural and microstructural properties. Thin Solid Films 515:5314–5323

Pan ZW, Dai ZR, Wang ZL (2001) Nanobelts of semiconducting oxides. Science 291:1947–1949

Philipose U, Sun P, Xu T, Ruda HE, Yang L, Kavanagh KL (2007a) Structure and photoluminescence of ZnSe nanostructures fabricated by vapor phase growth. J Appl Phys 101:014326(1)–014326(5)

Philipose U, Yang S, Xu T, Harry ER (2007b) Origin of the red luminescence band in photoluminescence spectra of ZnSe nanowires. Appl Phys Lett 90:063103

Singh V, Chauhan P (2009) Structural and optical characterization of CdS nanoparticles prepared by chemical precipitation method. J Phys Chem Solids 70:1074–1079

Solanki R, Huo J, Freeouf JL, Miner B (2002) Atomic layer deposition of ZnSe/CdSe superlattice nanowires. Appl Phys Lett 81:3864–3866

Tarey RD, Raju TA (1985) A method for the deposition of transparent conducting thin films of tin oxide. Thin Solid Films 128:181–189

Tauc J, Grigorovici R, Vancu A (1966) Optical properties and electronic structure of amorphous germanium. Phys Stat Solidi 15:627

Tian B, Zheng X, Kempa TJ, Fang Y, Yu N, Yu G, Huang J, Lieber CM (2007) Coaxial silicon nanowires as solar cells and nanoelectronic power sources. Nature 449:885–889

Williamson GK, Hall WH (1953) X-ray line broadening from field aluminum and wolfram. Acta Metall 1:22–31

Yang J, Wang G, Liu H, Park J, Cheng X (2009) Controlled synthesis and characterization of ZnSe nanostructures via a solvothermal approach in a mixed solution. Mater Chem Phys 115:204–208

Zhang XB, Ha KL, Hark SK (2001) Selenium-related luminescent centers in metalorganic chemical-vapor-phase deposition grown ZnSe epilayers on GaAs. Appl Phys Lett 79:1127(1)–1127(3)

Zhang XT, Ip KM, Li Q, Hark SK (2005) Photoluminescence of Ag-doped ZnSe nanowires synthesized by metalorganic chemical vapor deposition. Appl Phys Lett 86:203114(1)–203114(3)

Zhang H, Yang D, Ma X (2007a) Synthesis of flower-like CdS nanostructures by organic-free hydrothermal process and their optical properties. Mater Lett 61:3507–3510

Zhang T, Shen Y, Hu W, Sun J, Wu J, Ying Z, Xu N (2007b) Growth of ZnSe nanowires by pulsed-laser deposition. J Vac Sci Technol B 25:1823(1)–1823(4)